

The Open University's repository of research publications and other research outputs

Multiscale patterning of nanocomposite polyelectrolyte/nanoparticle films using inkjet printing and AFM scratching

Journal Item

How to cite:

Leigh, S. J.; Bowen, J. and Preece, J. A. (2015). Multiscale patterning of nanocomposite polyelectrolyte/nanoparticle films using inkjet printing and AFM scratching. *Materials Research Express*, 2(6), article no. 065301.

For guidance on citations see [FAQs](#).

© 2015 IOP Publishing Ltd

Version: Accepted Manuscript

Link(s) to article on publisher's website:
<http://dx.doi.org/doi:10.1088/2053-1591/2/6/065301>

Copyright and Moral Rights for the articles on this site are retained by the individual authors and/or other copyright owners. For more information on Open Research Online's data [policy](#) on reuse of materials please consult the policies page.

Materials Research Express



PAPER

Multiscale patterning of nanocomposite polyelectrolyte/nanoparticle films using inkjet printing and AFM scratching

RECEIVED
24 March 2015

REVISED
28 April 2015

ACCEPTED FOR PUBLICATION
7 May 2015

PUBLISHED
DD MM 2015

S J Leigh¹, J Bowen² and J A Preece³

¹ School of Engineering, University of Warwick, Coventry, CV4 7AL, UK

² School of Chemical Engineering, University of Birmingham, Edgbaston, B15 2TT, UK

³ School of Chemistry, University of Birmingham, Edgbaston, B15 2TT, UK

E-mail: s.j.leigh@warwick.ac.uk

Keywords: inkjet, polyelectrolyte, nanoparticle, atomic force microscopy, nanocomposite

Supplementary material for this article is available [online](#)

Abstract

The fabrication of structured polymer/nanoparticle composite films through a combination of additive, subtractive and self-assembly methodologies is investigated. Consumer grade inkjet printing hardware is employed to deposit cationic polyelectrolytes on (i) hydrophilic and (ii) hydrophobised glass substrates. The hydrophobisation process controls the spreading of the droplets and hence the lateral size of printed features. The printed cationic polyelectrolyte regions are used as a template to direct the self-assembly of negatively charged gold nanoparticles onto the surface. Micro-scale features are created in the polyelectrolyte/nanoparticle films using AFM scratching to selectively displace material. The effect of substrate wettability on film morphology is discussed.

1. Introduction

Inkjet printing (IJP) refers to processes where droplets of liquid ink are ejected from a reservoir through a micro-machined nozzle onto a surface to produce characters, codes or graphic patterns in adherence with a digital schematic. IJP technology is by far the most common form of printing technology for use by consumers wishing to transfer digital information into a paper copy while also being one of the most versatile, where printing media can range from paper and photographic paper, through to textiles and CD/DVD storage media [1, 2]. Because IJP technology is able to deposit well-defined volumes of liquid reproducibly across both absorbing and non-absorbing surfaces it has found many uses in the area of surface science and materials science for surface patterning and printed electronics [3]. IJP utilised in this manner falls into an expanding class of rapid fabrication and additive manufacturing technologies [4] where novel advanced and functional materials can be rapidly formed into functional structures and devices [5]. For instance IJP technology is utilised in macro-scale additive manufacturing to carry out the selective build-up of complex 3D structures [6].

Many bespoke IJP systems have been produced that deliver small volumes of liquid material to precise locations on surfaces [7, 8]. For instance, Murata *et al* presented a custom-made ultra-fine inkjet system as a tool for nanotechnology research which allowed arrangements of islands of material with a minimum size of less than one micron [9]. Using an ultra-fine silver paste, Murata achieved the direct print of an ultra-fine metallic wire of only a few micrometers in width without any pre-patterning treatment of the substrate. Furthermore, using the transition-metal nano-particles as catalyst-ink, patterned arrays of carbon nano-tubes were successfully obtained. A field emission from the patterned carbon nano-tubes was also confirmed. Calvert *et al* utilised both custom-made and adapted inkjet printers to print biopolymer and polymer materials in a layer-by-layer fashion to form insoluble complexes [10]. Inkjet printing is also utilised for reactive inkjet printing, where the expelled droplets are used as reactive building blocks in subsequent chemical reactions [11].

The major technical operations during IJP are (i) creation of an ink stream or droplets under pressure (created using thermal or piezoelectric stimulus), (ii) ejection of ink from a nozzle or orifice, (iii) control of drop size and uniformity and (iv) placement of drops on the printing surface. Control of these functions depends on

several design variables of the inkjet system, such as nozzle size, firing rate, drop deflection methods and ink viscosity. Precisely controlling these variables in a custom-made system can often prove technically challenging. Further, the cost of dedicated equipment can be prohibitive. Therefore, the ability to adapt a cheap, commercially available, consumer grade inkjet system where all these variables have been optimised is highly advantageous. When using consumer desktop inkjet printers fine control over the size of printed features beyond the default parameters is not always possible. Furthermore, lateral X-Y resolution is limited by the size of the dried droplets on the substrate. Typical inkjet features are on the order of tens of microns [12]. Hence methods that can be used to further enhance the lateral resolution of the technique while accessing different film morphologies are highly desirable. Mechanical scratching and shaving of surfaces of either bulk materials or thin films using an atomic force microscope (AFM) is a well-established technique for the production of micro-scale features on surfaces [13, 14]. The processes involve bringing an AFM tip into compressive normal contact with a surface and laterally moving the tip and substrate relative to one another, affording the accurate formation of trench like structures on the substrate surface.

Here we present a method that utilises consumer desktop inkjet equipment to deposit a cationically charged polyelectrolyte in a range of morphologies from individual islands through to dense films on glass substrates by simply selecting different shades of the same colour in desktop publishing software. Furthermore, the spreading of the polyelectrolyte on the substrates can be influenced by pre-treatment of the glass with a hydrophobic silane molecule. This pre-treatment stage allows a range of different film morphologies to be accessed combined with retarding lateral droplet spreading to create smaller 'island' features. After deposition the printed polyelectrolyte features can be further decorated by immersion into a complementary anionically charged Au nanoparticle solution causing the nanoparticles to selectively assemble onto the printed regions via attractive electrostatic interactions. Finally, the resultant composite films then undergo mechanical scratching using the sharp tip of an AFM to further define microscale features in the deposited 'islands'. The work presents a combination of both top-down and bottom-up methodologies to gain a versatile, yet simple technique for defining surface architectures.

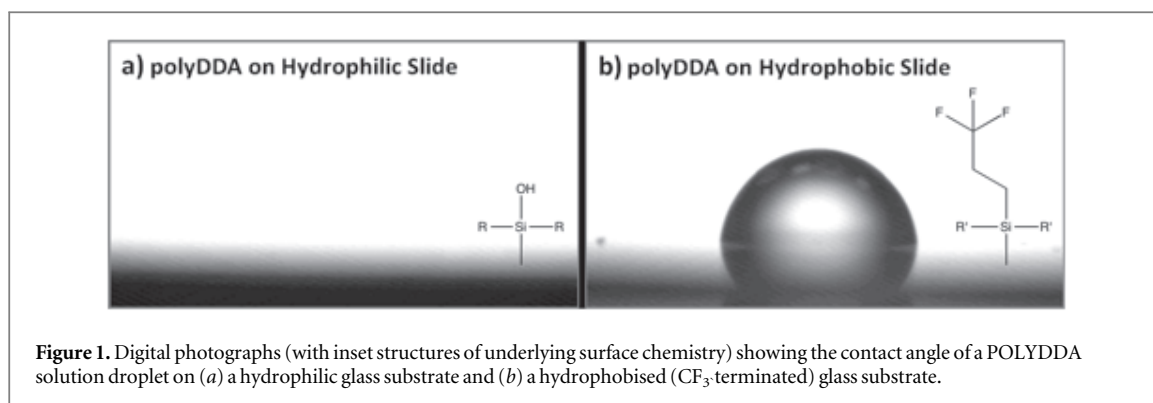
2. Results and discussion

2.1. Surface modification

While IJP is a useful technique for producing regular and repeatable drop sizes, when wanting to modify the lateral resolution of printed features there exists a need to control either the size of the droplet itself or the spreading of droplets on surfaces. On a consumer IJP system, modification of the droplet size is difficult, however surface modification of substrates to control droplet spreading can be carried out. In order to demonstrate this surface modification principle, glass slides were cleaned and used either as cleaned (hydrophilic) or immersed in a solution of trifluoropropylsilane (TFPS) for 2 h to render the glass slides hydrophobic [15]. The presence of the TFPS imparts hydrophobic character to the surface due to the presence of CF_3 from the trifluoropropyl groups ($-\text{Si}-(\text{CH}_2)_3\text{CF}_3$). After the TFPS deposition process, spectroscopic ellipsometry confirmed the presence of a 7.4 nm film on the surface of a section of Si wafer treated at the same time as the glass substrates. The thickness obtained indicates the presence of a TFPS multilayer structure as opposed to a single monomolecular layer (molecule length 0.7 ± 0.05 nm, terminal Cl to terminal F). By comparing the static contact angle of a 2 μL droplet of a NaCl solution of polydiallyldimethylammonium chloride (polyDDA) on a hydrophilic glass microscope slide (figure 1(a)) and on a TFPS terminated, hydrophobic glass slide (figure 1(b)), it was observed, as expected, that polyDDA exhibited a higher contact angle ($\sim 80^\circ$) on the hydrophobised surfaces compared to an untreated glass surface ($< 5^\circ$). The marked increase in contact angle for the CF_3 functionalised surface agreed with previous literature [16].

2.2. Inkjet printing

In order to carry out IJP of the polyDDA solution to the substrates, the CD printing tray of a consumer inkjet printer (Canon IP5300) was modified to retain standard glass microscope slides. The use of this tray and a printer with CD printing capability avoided the need for modification of any paper feeding mechanism to accept solid substrates. Inkjet printing of the polyDDA solution was carried out by cleaning and refilling the yellow print cartridge of the printer with the polyDDA solution. All of the yellow ink was removed from the cartridge using a combination of water and ethanol. By choosing an appropriate shade of yellow colour in MS PowerPoint it was possible to vary the amount of polyDDA deposited per unit area. The 4 shades of yellow used were termed, 1Y, 2Y, 3Y and 4Y with 1Y referring to the least amount of material deposited per unit area.



2.3. Nanoparticle deposition

In order to visualise the polyDDA regions printed on the glass surfaces and further derivatise the printed regions, the resultant substrates were immersed in a colloidal suspension of citrate-stabilised Au nanoparticles with an approximate diameter of 20 + 5 nm (Au-NP) at pH 4.5. Over time, the evolution of the characteristic dark red colour of Au-NP (from the nanoparticle *plasmon band*) on the polyDDA features was seen, which turned to a dark purple colour (from the nanoparticle *longitudinal plasmon band*). The colouration of the polyDDA/Au-NP features was not seen to increase past a deposition time of 1 h. The deposition kinetics of the Au-NP were recorded by monitoring the printed regions with a digital microscope and plotting the intensity of the blue pixels from the RGB image (see supporting information).

2.4. Analysis of printed features

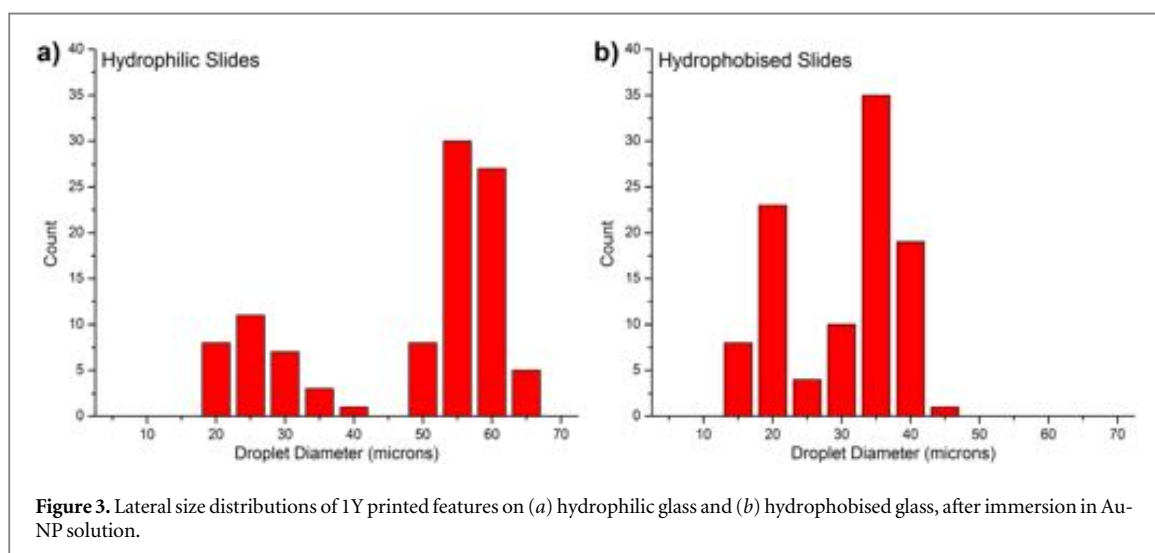
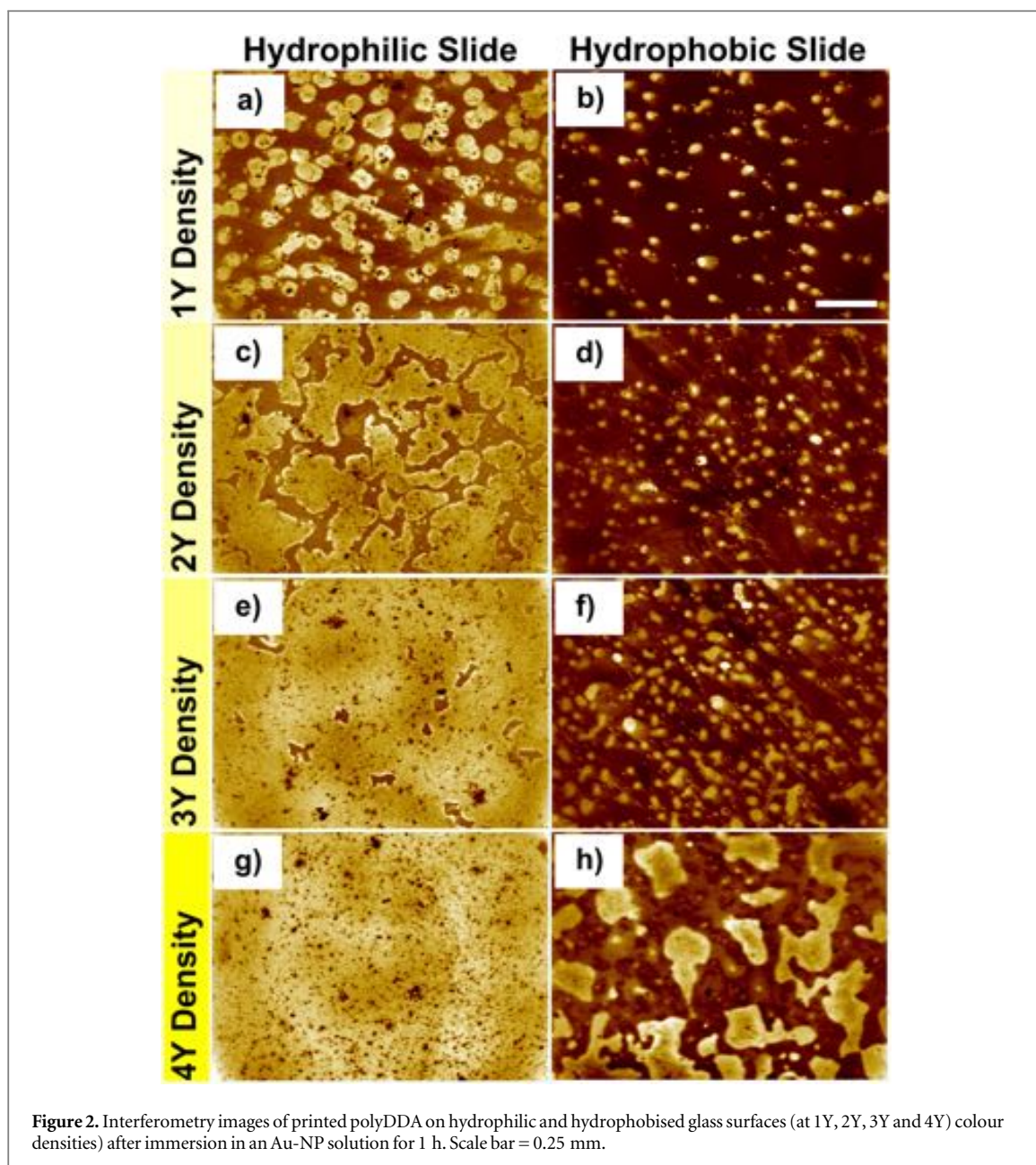
After 1 h, the samples were rinsed with UHP H₂O and dried under a stream of N₂. Figure 2 shows the resultant interferometry images of the hydrophilic and hydrophobised glass substrates after printing and immersion in Au-NPs. For the lowest print density (1Y), individual island domains were formed on both the hydrophilic and hydrophobised glass surfaces, however a difference in lateral size of the islands was observed between the two substrates (figures 2(a) and (b)). For the 2Y density, the hydrophilic glass surface exhibited extended island domains, apparently resultant from the coalescence of individual droplets. For the hydrophobised surfaces at 2Y, there are a greater number of individual domains but a reduction in droplet coalescence (figures 2(c) and (d)). For the 3Y density, the hydrophilic glass surface exhibits nearly full film coverage. The hydrophobised surfaces at this print density begin to show some droplet coalescence (figures 2(e) and (f)). At the highest print density (4Y), the hydrophilic glass surfaces exhibit full film coverage. The hydrophobised surfaces again exhibit increased coalescence (figures 2(g) and (h)).

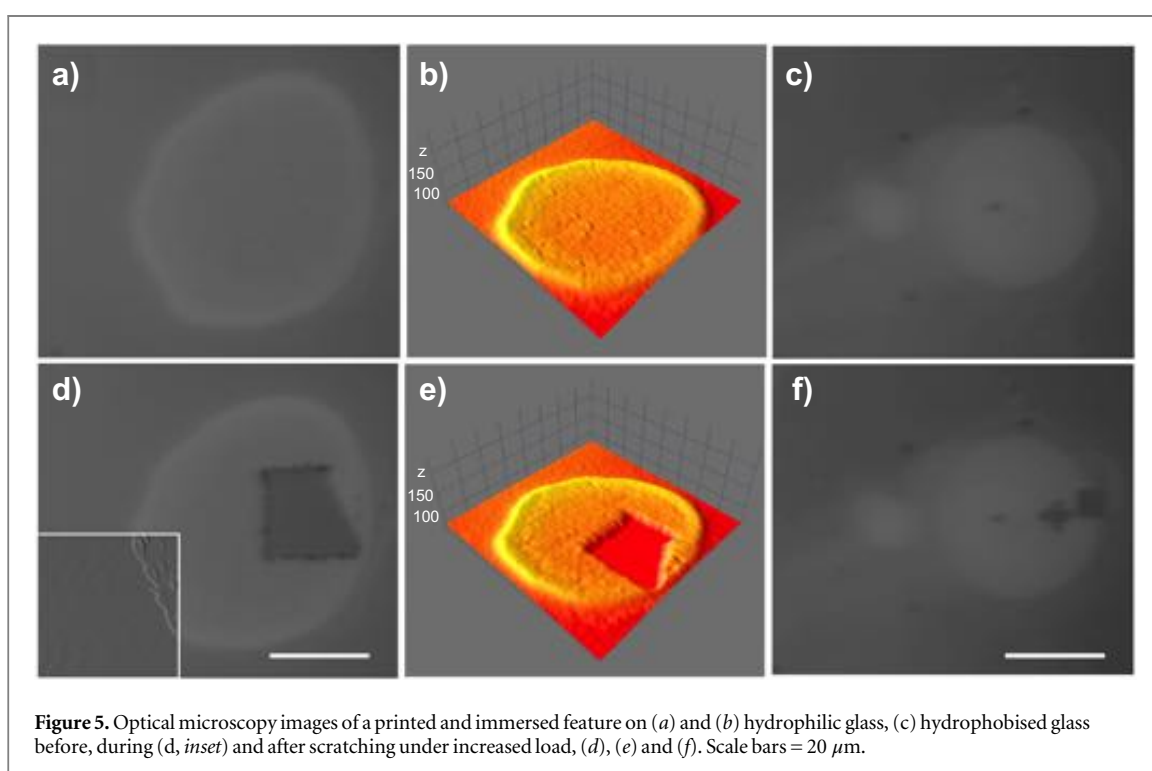
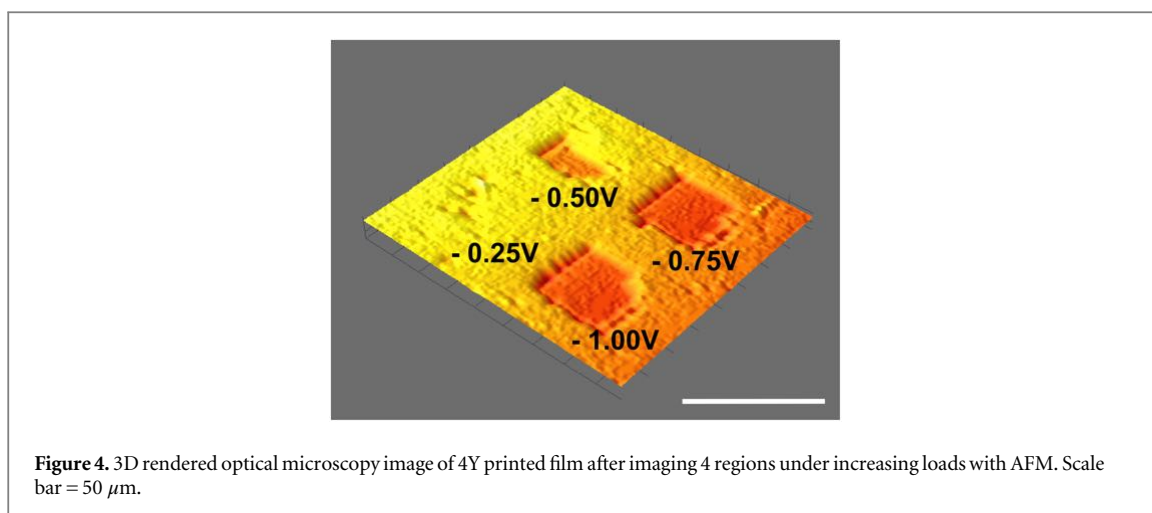
The interferometry images show that prior treatment of the printing surface can have a marked effect on the resultant printed features, allowing a number of different polyelectrolyte morphologies from discrete polyDDA islands to high surface coverage polyDDA films to be accessed. Features printed on hydrophilic and hydrophobised surfaces exhibited a range of thicknesses, typically in the range 30–60 nm.

A key observation from the interferometry analysis is the difference in lateral size of the 1Y printed regions on the hydrophilic glass and hydrophobised glass substrates. Size analysis of the features after immersion in Au-NPs was carried out using optical microscopy. The resultant histograms are presented in figure 3. On hydrophilic glass surfaces, the polyDDA/Au-NP features exhibited a bi-modal distribution with a large population of feature sizes between 50 and 60 μm . The second smaller feature population was centred around 21–25 μm . For the hydrophobised glass surfaces, a bi-modal distribution was observed, with high populations between 31 to 35 μm and 16 to 20 μm . This comparison reveals that as hypothesised, reduction in printed feature diameter is possible through simple modification of the underlying substrate surface chemistry.

2.5. Analysis of scratching

After evaluation of the surface modification, printing and nanoparticle assembly, AFM scratching was investigated as a route for creating well-defined structures within the IJP templated features. To carry out this process, 25 μm \times 25 μm square AFM images were scanned at compressive loads of 0.65, 1.30, 1.95 and 2.60 μN (corresponding to tip deflections of -0.25 V, -0.5 V, -0.75 V and -1.0 V respectively). The durability of a polyDDA/Au-NP film printed at 4Y density was tested (figure 4). Optical microscopy of the range of 1 μm regions revealed an optical contrast between the scanned and un-scanned regions, indicating material had been scratched away. Compressive loads of 1.95 and 2.60 μN gave rise to the most complete material displacement. Loads in the μN range agree with those observed previously for scratching-based removal of soft materials from hard substrates [17].





The scratched regions show a build-up of material in the top right hand corner and down the right hand side of the square features. This effect was also seen while monitoring the AFM image output during the scratching process. The build-up is believed to be some of the material removed under the motion of the tip and deposited at the edge of the feature as the AFM tip moves from right to left and from bottom to top. Attempts to subsequently re-image the scratched regions with the same AFM tip after the scratching were largely unsuccessful, with only poor quality, highly convoluted images obtained. The reasons for the poor imaging potential of the tip after scratching is thought to be blunting of the tip and material build-up on the tip causing increased interactions between the tip and remaining material on the surface [18]. The tips could however be re-used for further scratching operations without any obvious signs of degradation in scratching capability.

After determination of the force required to carry out the removal of material, the circular droplet features printed at 1Y density (on hydrophilic (figures 5(a) and (b)) and hydrophobic (figure 5(c)) surfaces) and immersed in Au-NPs, were subjected to AFM imaging at a load of 1.95 μN . After the scratching process, the droplets were imaged with the camera system of the AFM (figures 5(d) and (e)). As expected, the removal of material with the AFM tip had been replicated in the centre of the droplets, showing that it was possible to further modify fabricated features after IJP. The image recorded by the AFM during the scratching process is presented inset in figure 5(d) and shows the build-up of material towards the side of the scratched area. Beyond

simple squares, it was possible to create other features without the use of a dedicated lithography interface, by simply manipulating scan direction, aspect ratio and position (figure 5(f)).

3. Conclusions

Pre-treatment of a glass substrate with a fluorosilane hydrophobising agent, afforded the controlled spreading of printed droplets of aqueous polyelectrolyte solution. The regions of printed polyelectrolyte differed in their lateral dimensions from discrete 10–20 μm islands through to a high surface coverage film. Nanocomposite metal/organic films were created through templated self-assembly of gold nanoparticles onto the printed polyelectrolyte was achieved via attractive electrostatic interactions. The printed regions can be further patterned after derivatisation with gold nanoparticles by carrying out mechanical scratching within the discrete regions using atomic force microscopy. Features defined in this way could have interesting applications in areas such as nano-arrays and nano-fluidics.

4. Methodology

4.1. Cleaning of glass surfaces

Glass surfaces were cleaned by immersion of a fresh glass microscope slide in piranha solution for 30 min, followed by rinsing with UHP H_2O . The glass slides were then immersed in RCA solution for 1 h followed by rinsing and storage in UHP H_2O .

4.2. Hydrophobisation of glass surfaces

Glass surfaces were hydrophobised after the cleaning stage. Cleaned glass slides were immersed in a solution of trifluoropropylsilane (TFPS, 25 mM, EtOH) under ultrasonication for 2 h. After removal from the TFPS solution, the glass slides were twice rinsed with EtOH and CHCl_3 and sonicated in fresh EtOH. To aid in crosslinking of the silane layer, the slides were placed in an oven at 120 $^\circ\text{C}$ for 2 h. Ellipsometry was carried out using a spectroscopic ellipsometer (UVISEL, Horiba Jobin Yvon) on a chip of silicon wafer immersed in TFPS at the same time as the glass substrates. The ellipsometer was equipped with a broadband Xe light source. The angle of incidence and wavelength range was 70 $^\circ$ and 280–820 nm respectively. All measurements were made under conditions of ambient temperature, pressure and humidity. DeltaPsi software was used to determine the thickness of the film, which was modelled using the Cauchy equation.

4.3. Formulation of poly-diallyldimethylammonium chloride (polyDDA) solution and loading of ink cartridges

PolyDDA (20 mM) was added to an aqueous NaCl (0.1 M) solution. CLI-8Y (Yellow, Canon Inc.) ink cartridges had a hole drilled into the top of the reservoir and the majority of the yellow ink was removed with a needle and syringe. The cartridges were then rinsed extensively with UHP H_2O (resistivity = 18 $\text{M}\Omega\cdot\text{cm}$) to remove all the remaining yellow ink. To fill the cartridges with polyDDA solution, the remaining H_2O was removed with a syringe and then the cartridge was filled by syringe until with the polyDDA solution dripped out of the cartridge nozzle.

4.4. IJP of polyDDA

A commercially available inkjet printer (Canon Pixma ip5300) was used without modification. The CD printing tray for the printer was modified to accept standard size glass microscope slides. Prior to printing, fresh glass microscope slides were rinsed with ethanol and dried under a stream of N_2 . Prior to printing the polyDDA solution, the standard CLI-8Y print cartridge was removed and replaced with an H_2O filled cartridge and several pages of plain yellow printing were printed to remove final traces of the standard ink from the print head. When the H_2O filled cartridge was removed, it was replaced with the polyDDA filled cartridge and printing was commenced. polyDDA was printed at 4 different surface densities, corresponding to the four available shades of pure yellow within the software (1Y, 2Y, 3Y and 4Y). polyDDA was printed onto hydrophilic glass microscope slides then allowed to air dry at room temperature then stored in a desiccator.

4.5. Synthesis of citrate-stabilised gold nanoparticle solution (Au-NP)

A solution of citrate-stabilised gold nanoparticles was synthesised via the Frens method [19]. An aqueous solution of $\text{HAuCl}_4\cdot 3\text{H}_2\text{O}$ (40 mg, 49 mL) was heated under reflux for 5–10 min. An aqueous solution of sodium citrate (80 mg, 1 mL) was added. Heating under reflux was continued for a further 5 min to ensure complete reduction of the gold salt. The resultant colloidal solution was left to cool while stirring for 1 h. Finally,

the dark red solution was centrifuge three times for 10 min (3500 rpm) and the supernatant collected. Adjustment of the colloid pH to 4.5 was carried out using a minimal amount of HCl (0.06 M).

4.6. Solution deposition of Au-NP solution

Prior to deposition of the Au-NP solution, the polyDDA printed slides were rinsed with UHP H₂O for 1 min, then immersed into a concentrated citrate gold nanoparticle (Au-NP) solution.

4.7. AFM imaging and scratching

AFM imaging and scratching was carried out using a Veeco Dimension 3100 AFM operating in contact mode. Pyramidal tipped Si cantilevers (RTESP, Veeco Instruments, UK) were used for all experiments. For scratching experiments, scratching was performed at tip velocities of 40 $\mu\text{m s}^{-1}$ in contact mode, followed by tapping mode image acquisition of the scratched area.

4.8. Optical microscopy of features

Optical microscopy of the inkjet printed and scratched features was carried out using a combination of various different optical microscopy systems. For large scale magnified image analysis a Zeiss AxioScope fitted with 5X and 10X objectives was utilised. For analysis of scratched features and for sizing analysis, the calibrated optical system of the Dimension 3100 AFM was used.

4.9. Interferometry analysis of printed features

Surface topography analyses were performed using a MicroXAM2 interferometer (Omniscan, UK) operating with a white light source at a magnification of 50X.

Acknowledgments

The work carried out in this paper was funded by the grant FP6-NMP-14006 – ‘Precision Chemical Nanoengineering: Integrating Top-Down and Bottom-Up Methodologies for the Fabrication of 3D Adaptive Nanostructured Architectures’. The interferometer used in this research was obtained through Birmingham Science City: Innovative Uses for Advanced Materials in the Modern World (West Midlands Centre for Advanced Materials Project 2), with support from Advantage West Midlands (AWM) and part funded by the European Regional Development Fund (ERDF).

References

- [1] Calvert P 2001 Inkjet printing for materials and devices *Chem. Mater.* **13** 3299–305
- [2] Kiatkamjornwong S, Putthimai P and Noguchi H 2005 Comparison of textile print quality between inkjet and screen printings *Surf. Coat. Int. B: Coatings Transactions* **88** 25–34
- [3] Park E S, Chen Y, Liu T-J K and Subramanian V 2013 A new switching device for printed electronics: inkjet-printed microelectromechanical relay *Nano Lett.* **13** 5355–60
- [4] Zhang X, Jiang X N and Sun C 1999 Micro-stereolithography of polymeric and ceramic microstructures *Sensors Actuators* **77** 149–56
- [5] Leigh S J, Bradley R J, Pursell C P, Billson D R and Hutchins D A 2012 A simple, low-cost conductive composite material for 3D printing of electronic sensors *PLoS ONE* **7** e49365
- [6] Elliott A M, Ivanova O S, Williams C B and Campbell T A 2013 Inkjet printing of quantum dots in photopolymer for use in additive manufacturing of nanocomposites *Adv. Eng. Mater.* **15** 903–7
- [7] de Gans B-J, Duineveld P C and Schubert U S 2004 Inkjet printing of polymers: state of the art and future developments *Adv. Mater.* **16** 203–13
- [8] Wilson P, Lekakou C and Watts J F 2012 A comparative assessment of surface microstructure and electrical conductivity dependence on co-solvent addition in spin coated and inkjet printed poly(3,4-ethylenedioxythiophene):polystyrene sulphonate (PEDOT:PSS) *Organic Electronics* **13** 409–18
- [9] Murata K, Matsumoto J, Tezuka A, Matsuba Y and Yokoyama H 2005 Super-fine ink-jet printing: toward the minimal manufacturing system *Microsyst. Technol.* **12** 2–7
- [10] Calvert P, Skander L, Iyenger S and Patra P 2007 Inkjet printing of insoluble biopolymer and polymer complexes *PMSE Preprints* **48** 1023–4
- [11] Smith P J and Morrin A 2012 Reactive inkjet printing *J. Mater. Chem.* **22** 10965–70
- [12] Doggart J, Wu Y, Liu P and Zhu S 2010 Facile inkjet-printing self-aligned electrodes for organic thin-film transistor arrays with small and uniform channel length *ACS Applied Materials & Interfaces* **2** 2189–92
- [13] Diegoli S, Hamlett C A E, Leigh S J, Mendes P M and Preece J A 2007 Engineering nanostructures at surfaces using nanolithography *Proc. Inst. Mech. Eng. G, J. Aerosp. Eng.* **221** 589–629
- [14] Huang J-C, Li C-L and Lee J-W 2012 The study of nanoscratch and nanomachining on hard multilayer thin films using atomic force microscope *Scanning* **34** 51–9
- [15] Xiu Y, Zhu L, Hess D W and Wong C P 2007 Hierarchical silicon etched structures for controlled hydrophobicity/superhydrophobicity *Nano Lett.* **7** 3388–93
- [16] Xiu Y, Zhu L, Hess D W and Wong C P 2006 Biomimetic creation of hierarchical surface structures by combining colloidal self-assembly and Au sputter deposition *Langmuir* **22** 9676–81

- [17] Heyde M, Rademann K, Cappella B, Geuss M, Sturm H, Spangenberg T and Niehus H 2001 Dynamic plowing nanolithography on polymethylmethacrylate using an atomic force microscope *Rev. Sci. Instrum.* **72** 136–41
- [18] Carpick R W and Salmeron M 1997 Scratching the surface: fundamental investigations of tribology with atomic force microscopy *Chem. Rev.* **97** 1163–94
- [19] Frens G 1973 Controlled nucleation for the regulation of the particle size in monodisperse gold solution *Nat. Phys. Sci.* **241** 20–2

QUERY FORM

JOURNAL: Materials Research Express

AUTHOR: SJ Leigh *et al*

TITLE: Multiscale patterning of nanocomposite polyelectrolyte/nanoparticle films using inkjet printing and AFM scratching

ARTICLE ID: mrx514499

The layout of this article has not yet been finalized. Therefore this proof may contain columns that are not fully balanced/matched or overlapping text in inline equations; these issues will be resolved once the final corrections have been incorporated.

We have been provided funding information for this article as below. Please confirm whether this information is correct. Sixth Framework Programme: FP6-NMP-14006.

Page 7

Q1

Please check the details for any journal references that do not have a link as they may contain some incorrect information.
